

# Conductance distributions at the metal-insulator crossover in quasi 1-D pseudorandom wires

A. Cresti<sup>1</sup>, R. Farchioni<sup>2,a</sup>, and G. Grosso<sup>2</sup>

<sup>1</sup> NEST-INFM, Scuola Normale Superiore, Piazza dei Cavalieri 7, 56126 Pisa, Italy, and Dipartimento di Fisica “E. Fermi”, Università di Pisa, Largo B. Pontecorvo 3, 56127 Pisa, Italy

<sup>2</sup> NEST-INFM and Dipartimento di Fisica “E. Fermi”, Università di Pisa, Largo B. Pontecorvo 3, 56127 Pisa, Italy

Received 25 February 2005

Published online 8 August 2005 – © EDP Sciences, Società Italiana di Fisica, Springer-Verlag 2005

**Abstract.** A study of the distribution of conductances,  $P(g)$ , for quasi-one-dimensional (multichain) pseudorandom systems is here presented. We focus on the crossover between the metallic ( $\langle g \rangle \gtrsim 1$ ) and the insulating ( $\langle g \rangle \sim 0$ ) regimes with reference to the case of “cosine” and “tangent” pseudorandom potentials. The results are compared with those obtained for the truly random disordered systems with the same geometry. A rich variety of shapes of  $P(g)$  is thus evidenced in the crossover-transport regime and, in the case of identical interacting chains composing the device, we have shown that the conductance distribution of the system can be obtained from the results for the single pseudorandom chain.

**PACS.** 71.30.+h Metal-insulator transitions and other electronic transitions – 72.15.Rn Localization effects (Anderson or weak localization)

## 1 Introduction

Due to the random distribution of the scattering centers, the conductance  $g$  of quasi-1D *disordered systems* shows fluctuations from sample to sample, as it was discovered experimentally [1] and then confirmed theoretically [2–4]. These fluctuations, induced by quantum interference effects, may become independent of sample size and degree of disorder giving origin to the concept of Universal Conduction Fluctuations [3]. Therefore  $g$  is not a self-averaging quantity, i.e. it does not converge towards its ensemble average as a function of sample size; the most relevant information on charge transport is in general given by the statistical distribution of its values [5], which has been recently object of deep interest both in one dimensional [6, 7] and in quasi-one dimensional systems [8–10].

Two fundamental regimes with typical corresponding distributions,  $P(g)$ , have been individuated for disordered quantum wires: the metallic regime, with  $\xi \gg L$  and  $\langle g \rangle > 1$  ( $\xi$  is the localization length of the electronic states,  $L$  is the typical length of the system) and the insulating regime, with  $\xi \ll L$  and  $\langle g \rangle \ll 1$ . In the former case  $P(g)$  is a Gaussian function with log-normal tails [11,12], in the latter case  $P(g)$  is reproduced by a log-normal function [13].

More recently, beyond these two situations, an intermediate crossover regime has been object of deep interest: in fact the transition of  $P(g)$  from the log-normal shape to the Gaussian one is far from being smooth, as it was

demonstrated for disordered wires both in the absence and in the presence of time reversal symmetry [9,10], and for quasi-1D systems with corrugated surfaces [14].

In the tight binding scheme a disordered quantum wire is described, following the approach introduced by Anderson [15], by assigning random values to the site energies (or to the hopping interactions) of the Hamiltonian of the system. Quasi one dimensional (multichains) tight binding models with random diagonal or off-diagonal potential have been adopted as efficient tools to verify the extensibility to higher dimensions of the definitions and of the exact results obtained for strictly one dimensional disordered systems.

Beyond truly random values, other (deterministic) forms of aperiodicity have been introduced and studied with this method. Among them, a special interest has been devoted to *incommensurate lattices* [16–19], obtained assigning to the sites energies of the perfect crystal a periodic function with period incommensurate with respect to the lattice constant. The resulting configuration for such lattices has to be considered as intermediate between the ordered and the disordered ones.

By means of appropriate choices of the modulating potential functions, also *pseudorandom* sequences, i.e. neither periodic nor incommensurate, can be generated. These sequences are described by well defined functions of position (see e. g. Eqs. (3) and (4) below); their spectral properties in the strictly one dimensional case have shown interesting analogies and differences with respect to the corresponding random models mainly concerning the localization properties [20–26]. While pseudorandom

<sup>a</sup> e-mail: farchion@df.unipi.it

potentials in strictly 1-D chains have been widely studied in connection with the physics of chaos [21–23], for their localization properties [24, 25] and for the effect of the degree of pseudorandomness [26], to our knowledge no effort has been devoted to the study of the statistical properties of conductance in quasi one dimensional pseudorandom wires. In this paper we evaluate numerically the distribution of conductance, in the crossover between the metallic and the insulating regimes, in quantum wires where the lattice site energies are modulated by the two most widely studied pseudorandom potentials: the cosine and the tangent potentials. Our aim is to highlight the comparison of their spectral properties with the corresponding results of the truly random multichain system. Moreover, we show that if the coupled chains composing the system are identical, then the total distribution of conductances can be interpreted in terms of the results of the single chain.

The numerical approach we exploit is based on the tight binding Green's function formalism for the evaluation of the conductance [27, 28] of the quantum wire. We adopt a lattice model for the system Hamiltonian and the real-space renormalization procedure to reduce to manageable size the system composed by infinite (left and right) leads.

The paper is organized as follows: in Section 2 we describe the system and the theoretical methods adopted for the evaluation of conductances. Section 3 contains the results for the conductance distributions of pseudorandom quantum wires in the crossover between metallic and insulating regimes. Section 4 contains the conclusions.

## 2 Method and system details

Let the overall system composed by seminfinite (left and right) leads and a central wire be described by a square lattice. The quasi 1D structure under study can be represented by a strip of interacting chains with one  $1s$  orbital localized on each site. The Hamiltonian has the form  $H = H_L + H_R + H_D$  where  $H_L$  and  $H_R$  are the leads Hamiltonians:

$$H_{L(R)} = \sum_{i,j} \epsilon_{ij}^{L(R)} |\phi_i\rangle\langle\phi_j| \quad (1)$$

with  $\epsilon_{ii} = \epsilon_i = 0$  and  $\epsilon_{ij} = t$  if  $i \neq j$  nearest neighbors,  $\epsilon_{ij} = 0$  elsewhere;  $H_D$  is the device Hamiltonian

$$H_D = \sum_i \epsilon_i |\phi_i\rangle\langle\phi_i| + \sum_{i \neq j} t_{ij} |\phi_i\rangle\langle\phi_j|, \quad (2)$$

$|\phi_i\rangle$  denotes the  $s$ -like orbital centered on the site  $i = (n, \alpha)$ , the index  $n$  labels the sites along the chains and  $\alpha$  refers to the chain number;  $\epsilon_i$  are the site energies and  $t_{ij}$  the hopping interactions between the sites. We limit here to first neighbour interactions and indicate with  $t_{\parallel} = t_{n\alpha, n\pm 1\alpha}$  and  $t_{\perp} = t_{n\alpha, n\alpha\pm 1}$  the intrachain and interchain interactions, respectively; moreover we fix  $t_{\parallel} = t_{\perp} = t$  (which is chosen as energy unit) both in the leads and in the device.

The site energies of the leads are chosen equal to zero and the site energies for each chain in the device are assigned according to the following pseudorandom potentials:

$$V_n = W \cos(2\pi\eta n^\nu) \quad (3)$$

and

$$V_n = W \tan(2\pi\eta n^2). \quad (4)$$

In expressions (3) and (4)  $\eta$  is an irrational number and  $\nu > 1$ . When we operate in the truly pseudorandom potential regime, we fix conventionally the origin of the device at the site  $n = 10^5$ ; moreover to have different configurations for different chains we assign the site energies  $\epsilon_{n\alpha}$  shifting the site index  $n$  in the forms (3) and (4) by  $10^5$  sites for each chain, for different  $\alpha$  label. The irrational number  $\eta$ , which is irrelevant in the pseudorandom case we are considering, is fixed by the relation  $2\pi\eta = 1.1$ .

The main difference between expressions (3) and (4) resides in the fact that in the former case the pseudorandomness is due to the rapid oscillation of the modulation [25], while in the latter this behavior is also enriched by the unboundness of the function which determines very strong fluctuations in the amplitude of site energies. In the cosine potential (3) the degree of pseudo-randomness is driven by the parameter  $\nu$  [24]: for  $1 < \nu < 2$  the localization of the electronic states is weak and the presence of a single delocalized state has been predicted at  $E = 0$  [25]; for  $\nu > 2$  the localization is complete and, for  $\nu > 3$ , tests for randomness used in computer science have given results undistinguishable to a random sequence [26].

The tangent potential (4) has been often studied in connection with the periodically kicked quantum rotor problem [21–23]. When it is assigned to the sites of a 1D chain, the resulting lattice presents the same localization properties as the Lloyd model [29], where the random site energies are distributed according to the Cauchy distribution; moreover, the Lloyd and the tangent models show the same analytic energy dependence of the Lyapunov coefficient [30].

The calculation of the conductances of the multichain wires has been performed by means of the Keldysh-Green function theory used in quantum transport [27, 28]; the great advantage of this approach is the possibility to evaluate the space and energy distribution of the steady state currents that flow in a device biased at different chemical potentials, by means of standard retarded Green's functions. Moreover, the effect of the leads and of external perturbations are easily inserted in the procedure. The conductance at the chemical potential  $\mu$  ( $\mu_L \sim \mu_R \sim \mu$ ) has the form [31]:

$$g(\mu) = \frac{2e^2}{h} \text{Tr} \{ \Gamma_{11}^{(left)}(\mu) G_{1M}^R(\mu) \Gamma_{MM}^{(right)}(\mu) G_{M1}^A(\mu) \}. \quad (5)$$

where 1 and  $M$  are border column sites of the device. The linewidth matrices  $\Gamma$  are given by

$$\Gamma_{11}^{(left)} = i t_{10} (g_{00}^R - g_{00}^A) t_{01}, \quad (6)$$

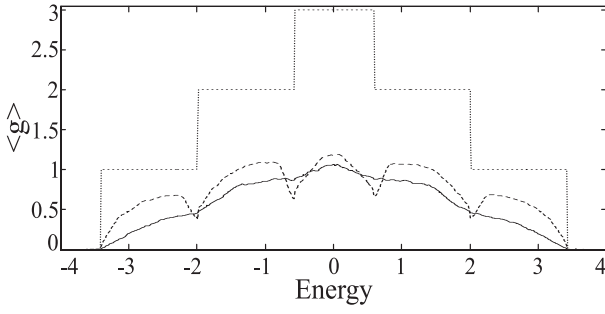


**Fig. 1.** Average conductance as a function of the Fermi energy of three interacting chains of length  $L=30$ . Site energies along the chains are assigned according the cosine potential (3) with  $W=0.5$  and  $\nu = 3.5$ . The full line corresponds to chains with identical energies for sites with the same index; the dashed line to the case of different chains with different site energies (see text). The dotted line indicates the conductance of three perfect chains with ( $\varepsilon_i = 0$  and  $t_{ij} = -1$ ). Averages are performed over 1000 configurations

and

$$\Gamma_{MM}^{(right)} = i t_{M,M+1} (g_{M+1,M+1}^R - g_{M+1,M+1}^A) t_{M+1,M}, \quad (7)$$

and are built in terms of the hopping interactions between leads and device and of the retarded and advanced equilibrium Green functions  $g^R$  and  $g^A$  of the left and right (isolated) leads. All the quantities that appear in the form (5) can be calculated with a real-space renormalization procedure, by recursively eliminating columns of sites [32].

## 3 Results

### 3.1 Interacting chains with identical site energies

Before considering the truly pseudorandom system composed by different chains, we study here a device composed by identical interacting chains (i.e. with identical energies at corresponding sites) because this allows us to obtain analytic results in terms of the conductance distribution of the single isolated chain. For sake of simplicity, we consider here the case of three coupled chains. Figure 1 reports the conductance averaged over 1000 configurations,  $\langle g \rangle$ , as a function of the Fermi energy for three identical interacting chains of length  $L = 30$  whose site energies are assigned according to the sequence (3) with  $W=0.5$ ,  $\nu = 3.5$  (full line). In comparison we report on the same figure the conductance of three perfect chains with  $\varepsilon_i = 0$  and  $t_{ij} = t_{\perp} = -1$  (dotted line), and the average conductance of three chains of the same length ( $L = 30$ ) whose site energies are defined according to the sequence (3) but with the counting index  $n$  shifted by  $10^5$  sites for each chain, so to obtain three pseudorandom different chains.

We consider now the conductance distribution, *in the crossover regime*, for the three identical coupled chains introduced before. Starting from interacting chains with the same site energies at the corresponding sites, a new orthonormal basis can be found which allows to decouple

the system into a set of non interacting chains with the same intrachain hopping  $t_{\parallel}$  and new diagonal elements. In the case of three interacting chains the new basis  $\{|\phi'_{n\alpha}\rangle\}$  and the corresponding new diagonal elements  $\varepsilon'_{n\alpha}$  have the following expressions:

$$|\phi'_{n1}\rangle = \frac{|\phi_{n1}\rangle + \sqrt{2}|\phi_{n2}\rangle + |\phi_{n3}\rangle}{2} \quad (\varepsilon'_{n1} = \varepsilon_{n1} + \sqrt{2}t_{\perp})$$

$$|\phi'_{n2}\rangle = \frac{|\phi_{n1}\rangle - \sqrt{2}|\phi_{n2}\rangle + |\phi_{n3}\rangle}{2} \quad (\varepsilon'_{n2} = \varepsilon_{n2} - \sqrt{2}t_{\perp})$$

$$|\phi'_{n3}\rangle = \frac{|\phi_{n1}\rangle - |\phi_{n3}\rangle}{\sqrt{2}} \quad (\varepsilon'_{n3} = \varepsilon_{n3})$$

where  $\{|\phi_{n\alpha}\rangle\}$ ,  $\varepsilon_{n\alpha}$  and  $t_{\perp}$  have been defined for the Hamiltonian (2). If we put  $t_{\parallel} = -1$ , the conductance of these three new non interacting chains is different from zero in the energy intervals  $(-2 - \sqrt{2}, 2 - \sqrt{2})$ ,  $(-2, 2)$  and  $(-2 + \sqrt{2}, 2 + \sqrt{2})$ , respectively. The total conductance  $g(E)$  can be written in terms of the conductances  $\tilde{g}(E)$  of the single chains as  $g(E) = \tilde{g}(E) + \tilde{g}(E + \sqrt{2}) + \tilde{g}(E - \sqrt{2})$ ; as a consequence, in the interval  $(-2 + \sqrt{2}, 2 - \sqrt{2})$  the contributions of the three chains are summed; in the intervals  $(-2, -2 + \sqrt{2})$  and  $(2 - \sqrt{2}, 2)$  only two chains contribute to  $g(E)$ , and in the intervals  $(-2 - \sqrt{2}, -2)$  and  $(2, 2 + \sqrt{2})$  just one chain contributes to  $g(E)$ .

In these energy intervals the total conductance distributions  $P(g, E)$  can be evaluated in terms of the distributions  $p(g, E)$  of the single chains: in the external energy intervals  $(-2 - \sqrt{2}, -2)$  and  $(2, 2 + \sqrt{2})$  the total distribution coincides with the distributions of the single chain with energy translated by  $\sqrt{2}$  and  $-\sqrt{2}$ , respectively; in the internal intervals, where two and three channels are active for the conductance of the system,  $P(g, E)$  is an appropriate convolution of the contributions of the single chains. The normalization condition adopted is  $\sum_i P(g_i) = 1$ . Figures 2, 3 and 4 report histograms built from  $P(g_i)$  with  $g_i$  separated by  $\Delta g=0.01$ ; thus the total area under the curves is 0.01. The above considerations can be summarized in the following analytic expressions:

$$P(g, E) = p(g, E + \sqrt{2}) \quad (-2 - \sqrt{2} < E < -2)$$

$$P(g, E) = \sum_{0 < g' < g} p(g', E) p(g - g', E + \sqrt{2}) \quad (-2 < E < \sqrt{2} - 2)$$

$$P(g, E) = \sum_{0 < g' < g} p(g', E) \sum_{0 < g'' < g - g'} p(g'', E + \sqrt{2}) p(g - g' - g'', E - \sqrt{2}) \quad (|E| < 2 - \sqrt{2})$$

$$P(g, E) = \sum_{0 < g' < g} p(g', E) p(g - g', E - \sqrt{2}) \quad (2 - \sqrt{2} < E < 2)$$

$$P(g, E) = p(g, E - \sqrt{2}) \quad (2 < E < 2 + \sqrt{2}).$$

In Figure 2 we report a comparison between the results obtained from the above expressions and the numerical

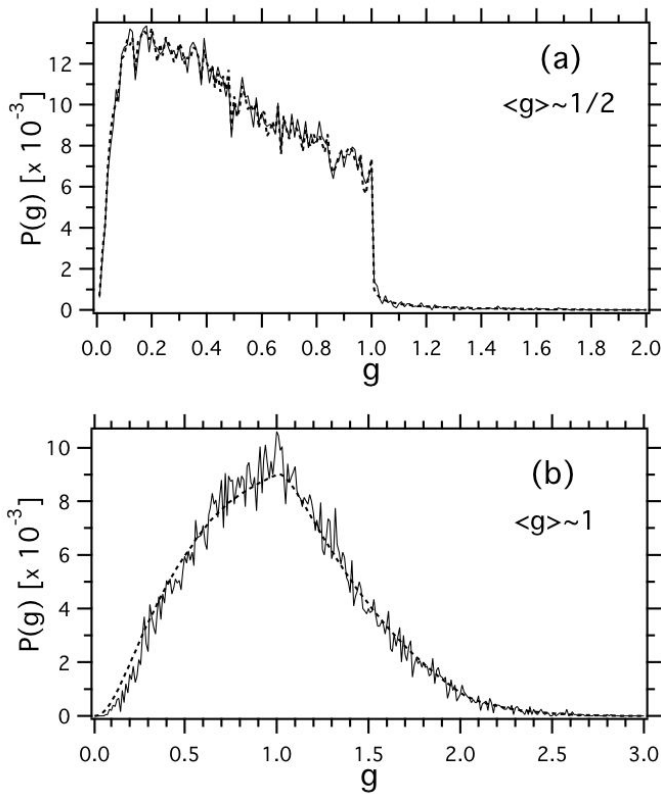


**Fig. 2.** Comparison between the convolution of single chain distributions (dashed lines) and numerical results (full lines) for the conductance distributions of three interacting identical chains of length  $L = 30$ . Site energies are assigned according to the potential (3) with  $W = 0.5$  and  $\nu = 3.5$ . In (a)  $E = 1.99$ ,  $\langle g \rangle \sim 1/2$ , in (b)  $E = 0.25$ ,  $\langle g \rangle \sim 1$ .

results (the averages are calculated over 20000 configurations) for the total conductance distributions  $P(g, E)$  evaluated at an energy chosen in the second interval ( $E = 1.99$ ,  $\langle g \rangle \sim 1/2$ , Fig. 2a) and at an energy in the most internal interval ( $E = 0.25$ ,  $\langle g \rangle \sim 1$ , Fig. 2b). The results found for the most external energy intervals are practically coincident. It can be seen that also for this simple identical three-chains system, the results in the crossover regime are highly non trivial being very different from standard Gaussian or log-normal distributions.

### 3.2 Interacting chains with different site energies

We consider here the case of coupled chains with independent pseudorandom site energies distributions; we have numerically evaluated the shape of conductance distributions  $P(g)$  for different values of  $\langle g \rangle$  obtained for several geometrical configurations and strength parameters which define the pseudorandom potentials (3) and (4). The method based on the Green's function described in Section 2 allows to handle easily systems composed by more than hundred chains. We here limit ourself to the case of three chains for comparison with the results on random systems present in the literature [10]. The results

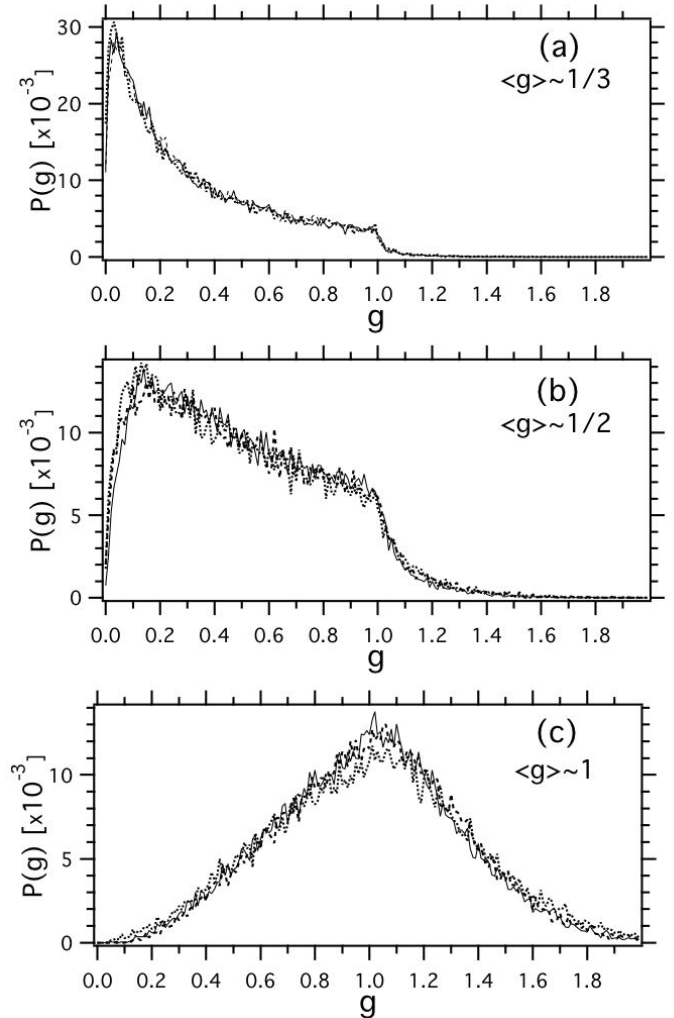


**Fig. 3.** Conductance distribution for three coupled chains with independent site energies. (a)  $\langle g \rangle \sim 1/3$  (full line: potential (3),  $N=7$ ,  $L=47$ ,  $\nu=2.5$ ,  $W=1.0$ ; dashed line: potential (3),  $N=5$ ,  $L=142$ ,  $\nu=1.8$ ,  $W=0.5$ ; dotted line: potential (4),  $N=11$ ,  $L=68$ ,  $W=0.3$ ). (b)  $\langle g \rangle \sim 1/2$  (full line: potential (3),  $N=3$ ,  $L=79$ ,  $\nu=2.5$ ,  $W=0.5$ ; dashed line: potential (3),  $N=5$ ,  $L=30$ ,  $\nu=1.8$ ,  $W=1.0$ ; dotted line: potential (4),  $N=7$ ,  $L=52$ ,  $W=0.2$ ). (c)  $\langle g \rangle \sim 1$  (full line: potential (3),  $N=3$ ,  $L=38$ ,  $\nu=2.5$ ,  $W=0.5$ ; dashed line: potential (3),  $N=5$ ,  $L=57$ ,  $\nu=1.8$ ,  $W=0.5$ ; dotted line: potential (4),  $N=20$ ,  $L=39$ ,  $W=0.4$ ). The plots are obtained for  $E = 0$  and  $2\pi\eta=1.1$

presented below have been obtained from 20000 generated configurations.

For both potentials we have found a non trivial transition of  $P(g)$  from the Gaussian to the log-normal distribution. In particular, for  $\langle g \rangle \sim 1/3$  (see Fig. 3a)  $P(g)$  grows steeply and beyond a pronounced peak shows a decreasing behaviour up to  $g \sim 1$ . A similar behavior is observed also for  $\langle g \rangle \sim 1/2$  (Fig. 3b) where the peak on the left is less pronounced and shifted to the right in the conductance scale. For  $\langle g \rangle \sim 1$ , the form of  $P(g)$  at  $g \sim 1$  presents a cusp shape due to the matching of the left part of the plot with the exponentially decreasing right

part (Fig. 3c). These calculations extend the validity of the analytic results [33–35] found in the case of *disordered* quantum wires, which predict a sharp (exponential) drop in the distributions for  $g > 1$ . The plots reported in Figure 3 show that although the lattices considered have pseudorandom distributions generated by the different laws (3) and (4), and consequently show different localization properties, anyhow they present similar conductance distributions with shapes similar to the ones of the (corresponding) random wires [10]. Moreover, from different choices of the parameters defining the potentials (3) and (4), but still remaining in the pseudorandom regime, we have evidenced that the shapes of  $P(g)$  can be deeply different from the genuinely random case. As a first example we consider the potential (3) with  $\nu = 1.5$  and choose the geometrical and potential parameters so to have  $\langle g \rangle \sim 1/2$ : if the number of interacting chains is  $N = 3$  and the amplitude  $W = 0.5$ , we can see (dotted line in the Fig. 4a) that the peak observed in Fig. 3b at  $g \gtrsim 0$  is absent, and the plot of  $P(g)$  shows a sharp increase as  $g \rightarrow 0$ . This behavior changes increasing  $W$  ( $W=1.0$ , dashed line) and the number of interacting chains ( $N = 7, W = 1.5$ ; full line) still conserving the value  $\langle g \rangle \sim 1/2$ : in these cases the shapes of  $P(g)$  are similar to those reported in Figure 3b. The curves shown in Figure 4a stress once again that the pseudorandomness of the potential (3) is governed by the parameter  $\nu$  and that differences in localization and transport properties with respect to the random case can be relevant. Moreover, when the length  $L$  of the wire is enough to simulate a one dimensional system (as in the case  $N = 3$  and  $L = 238$ ), the distribution of  $P(g)$  assumes, in the region  $g \sim 0$ , a shape which resembles the left branch of the typical U-shaped form for a single chain with the same site potential parameters.

Similar results are found for the tangent potential (4): in Figure 4b a transition from an initially decreasing behaviour of the shape of  $P(g)$  for  $N = 3, W = 0.2$  (dotted line), to a behaviour closer to the plots of Figure 3b is reached for  $N = 5, W = 0.3$  (dashed line) and for  $N = 7, W = 0.3$  (full line). Also in this case for large  $L$  the conductance distribution for  $g \sim 0$  increases sharply; moreover, we remark that this behavior of  $P(g)$  regards the part of the plots around  $g \sim 0$ , while the exponential decrease of  $P(g)$  beyond  $g \sim 1$  is reproduced by the analytic and numerical results valid for the random case [33–37].

## 4 Conclusions

In the crossover region between the metallic ( $\langle g \rangle \gtrsim 1$ ) and insulating ( $\langle g \rangle \ll 1$ ) regimes, we have calculated the conductance distributions of multichain quantum wires described by a tight binding scheme with site energies assigned according to pseudorandom sequences. We have found that the shape of the distributions of conductances is neither Gaussian nor log-normal; in fact they show an initial increasing behavior for  $g \gtrsim 0$  and an exponential decrease for  $g > 1$ , if  $\langle g \rangle \lesssim 1$ , while for  $\langle g \rangle \sim 1$  a cusp shape is observed at  $g \sim 1$ . These features have been observed also for the case of identical interacting

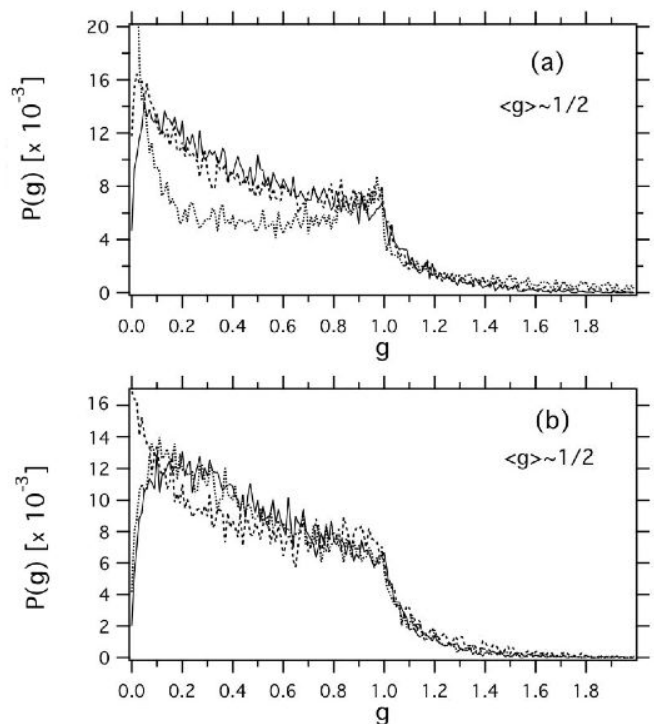


**Fig. 4.** (a) Conductance distributions for potential (3),  $\nu = 1.5$ , and  $\langle g \rangle \sim 1/2$  (full line:  $N = 7, L = 19, W = 1.5$ ; dashed line:  $N = 3, L = 23, W = 1.0$ ; dotted line:  $N = 3, L = 238, W = 0.5$ ). (b) Conductance distribution for potential (4),  $\langle g \rangle \sim 1/2$  (full line:  $N = 7, L = 52, W = 0.3$ ; dashed line:  $N = 5, L = 38, W = 0.3$ ; dotted line:  $N = 3, L = 23, W = 0.2$ ). The plots are obtained for  $E = 0$  and  $2\pi\eta = 1.1$ .

pseudorandom chains where the conductance distribution of the device can be obtained from the results for the single chain. Moreover, differently from the random case, a sharp increase of  $P(g)$  at  $g \sim 0$  has been evidenced both for the cosine and the tangent models in analogy with the strictly one-dimensional isolated chain.

This work has been supported by the National Enterprise for Nanoscience and Nanotechnology (NEST).

## References

1. C.P. Umbach, S. Washburn, R.B. Laibowitz, R.A. Webb, Phys. Rev. B **30**, 4048 (1984)
2. A.D. Stone, Phys. Rev. Lett. **54**, 2692 (1985)
3. P.A. Lee, Stone, Phys. Rev. Lett. **55**, 1622 (1985)
4. B.L. Alt'schuler, Pis'ma Zh. Eksp. Teor. Fiz. **41**, 530 (1985) [Sov. Phys. JETP Lett. **41**, 648 (1985)]
5. D. Belitz, S. Kirkpatrick, Rev. Mod. Phys. **66**, 261 (1994); P. Lee, T.V. Ramakrishnan, Rev. Mod. Phys. **57**, 287 (1985); C.W.J. Beenaker, Rev. Mod. Phys. **69**, 731 (1997)
6. L.I. Deych, A.A. Lisyansky, B.L. Altschuler, Phys. Rev. Lett. **84**, 2678 (2000); L.I. Deych, A.A. Lisyansky, B.L. Altschuler, Phys. Rev. B **64**, 224202 (2001)
7. H. Schomerus, M. Titov, Eur. Phys. J. B **35**, 421 (2003)
8. A.V. Tartakowski, Phys. Rev B **52**, 2704 (1995)

9. V. Plerou, Z. Wang, Phys. Rev. B **58**, 1967 (1998)
10. L.S. Froufe-Pérez, A. García-Mochales, P.A. Serena, P.A. Mello, J.J. Sáens, Phys. Rev. Lett. **89**, 246403 (2002)
11. B.L. Alt'schuler, V.E. Kravstov, I.V. Lerner, Zh. Eksp. Teor. Fiz. **91**, 2276 (1986) [Sov. Phys. JETP **64**, 1352 (1986)]
12. V.E. Kravstov, I.V. Lerner, V.I. Yudson, Zh. Eksp. Teor. Fiz. **94**, 255 (1988) [Sov. Phys. JETP **68**, 1441 (1988)].
13. A.A. Abrikosov, Solid State Commun. **37**, 997 (1981)
14. A. García-Martin, J.J. Saenz, Phys. Rev. Lett. **87**, 116603 (2001)
15. P.W. Anderson, Phys. Rev. **109**, 1492 (1958)
16. J.B. Sokoloff, Phys. Rep. **126**, 189 (1985)
17. S. Aubry, G. André, Ann. Israel Phys. Soc. **3**, 133 (1979)
18. S. Das Sarma, Song He, X.C. Xie, Phys. Rev. Lett. **61** 2144 (1988); S. Das Sarma, Song He, X.C. Xie, Phys. Rev. B **41**, 5544 (1990)
19. R. Farchioni, G. Grosso, G. Pastori Parravicini, Phys. Rev. B **45**, 6383 (1992); R. Farchioni, G. Grosso, G. Pastori Parravicini, Phys. Rev. B **47**, 2394 (1993)
20. K. Ishii, Suppl. Prog. Theor. Phys. **53**, 77 (1973)
21. S. Fishman, D.R. Grempel, R.E. Prange, Phys. Rev. Lett. **49**, 509 (1982)
22. D.R. Grempel, R.E. Prange, S. Fishman, Phys. Rev. A **29** 1639 (1984)
23. S. Fishman, R.E. Prange, M. Griniasty, Phys. Rev. A **39**, 1628 (1989)
24. M. Griniasty, S. Fishman, Phys. Rev. Lett. **60**, 1334 (1988)
25. D.J. Thouless, Phys. Rev. Lett. **61**, 2141 (1988)
26. N. Brenner, S. Fishman, Nonlinearity **5**, 211 (1992)
27. L.V. Keldysh, Zh. Eksp. Teor. Fiz. **47**, 1515 (1964) [L.V. Keldysh, Sov. Phys. JEPT **20**, 1018 (1964)]
28. C. Caroli, R. Combescot, P. Nozières, D. Saint-James, J. Phys. C **4**, 916 (1971); C. Caroli, R. Combescot, P. Nozières, D. Saint-James, J. Phys. C **5**, 21 (1972)
29. P. Lloyd, J. Phys. C **2**, 1717 (1969)
30. D.J. Thouless, J. Phys. C **5**, 77 (1972)
31. A. Cresti, R. Farchioni, G. Grosso, G. Pastori Parravicini, Phys. Rev. B **68**, 075306 (2003)
32. See for instance G. Grosso, G. Pastori Parravicini, *Solid State Physics* (Academic Press, London 2000)
33. K.A. Muttalib, P. Wölfle, Phys. Rev. Lett. **83**, 3013 (1999)
34. V.A. Gopar, K.A. Muttalib, P. Wölfle, Phys. Rev. B **66**, 174204 (2002)
35. K.A. Muttalib, P. Wölfle, A. García-Martin, V.A. Gopar, Europhysics Lett. **61**, 95 (2003)
36. M. Rühländer, P. Marcos, C.M. Soukoulis, Phys. Rev. B **64**, 212202 (2001)
37. P. Marcos, Phys. Rev. B **65**, 104207 (2002)